

Edge-Sharing Biocatahedral Diruthenium(III) Complexes Containing Methoxy and Carboxylate Bridges: X-ray Structures, Redox Behavior, and Core Stability[†]

Chellamma Sudha, Sisir K. Mandal, and Akhil R. Chakravarty*

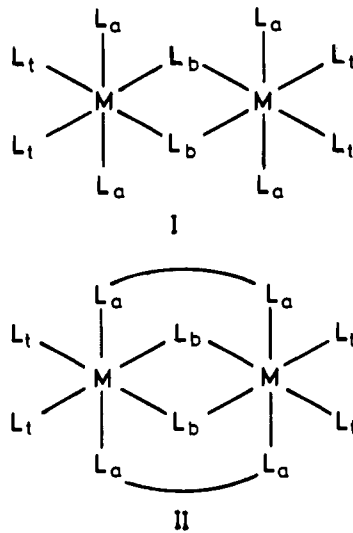
Department of Inorganic and Physical Chemistry, Indian Institute of Science, Bangalore-560 012, India

Received March 16, 1994[‡]

Edge-sharing biocatahedral (ESBO) complexes $[Ru_2(OMe)(O_2CC_6H_4-p-X)_3(1-MeIm)_4](ClO_4)_2$ ($X = OMe$ (**1a**), Me (**1b**)) and $[Ru_2(O_2CC_6H_4-p-X)_4(1-MeIm)_4](ClO_4)_2$ ($X = OMe$ (**2a**), Me (**2b**)) are prepared by reacting $Ru_2Cl(O_2CR)_4$ with 1-methylimidazole (1-MeIm) in methanol followed by treatment with $NaClO_4$. Complex **2a** and the PF_6^- salt (**1a'**) of **1a** have been structurally characterized. Crystal data for **1a'**: $1.5MeCN \cdot 0.5Et_2O$: triclinic, $P\bar{1}$, $a = 13.125(2)$ Å, $b = 15.529(3)$ Å, $c = 17.314(5)$ Å, $\alpha = 67.03(2)^\circ$, $\beta = 68.05(2)^\circ$, $\gamma = 81.38(1)^\circ$, $V = 3014(1)$ Å³, $Z = 2$. Crystal data for **2a**: triclinic, $P\bar{1}$, $a = 8.950(1)$ Å, $b = 12.089(3)$ Å, $c = 13.735(3)$ Å, $\alpha = 81.09(2)^\circ$, $\beta = 72.27(1)^\circ$, $\gamma = 83.15(2)^\circ$, $V = 1394(1)$ Å³, $Z = 1$. The complexes consist of a diruthenium(III) unit held by two monoatomic and two three-atom bridging ligands. The 1-MeIm ligands are at the terminal sites of the $[Ru_2(\mu-L)(\eta^1:\mu-O_2CR)(\eta^1:\eta^1:\mu-O_2CR)_2]^{2+}$ core having a Ru—Ru single bond ($L = OMe$ or η^1-O_2CR). The Ru—Ru distance and the Ru—O—Ru angle in the core of **1a'** and **2a** are 2.49 Å and ~76°. The complexes undergo one-electron oxidation and reduction processes in $MeCN - 0.1$ M TBAP to form mixed-valence diruthenium species with Ru—Ru bonds of orders 1.5 and 0.5, respectively.

Introduction

Edge-sharing biocatahedral (ESBO) complexes form an important class in the chemistry of complexes containing metal–metal multiple bonds.^{1–6} The ESBO complexes, in general, belong to the structural types I and II. The metal–metal interactions depend primarily on the electronic configuration



of the transition-metal ion, on the type of monoatomic bridging ligands (L_b), and on the presence or absence of any three-atom bridging ligands at the axial positions (L_a = axial ligand; L_t = terminal ligand). Among the ESBO M_2L_{10} systems, the dichloro-bridged complexes have been extensively studied.^{1,2}

In this paper we report the ESBO diruthenium(III) complexes $[Ru_2(OMe)(O_2CR)_3(1-MeIm)_4](ClO_4)_2$ (**1**) and $[Ru_2(O_2CR)_4(1-MeIm)_4](ClO_4)_2$ (**2**) ($R = C_6H_4-p-X$; $X = OMe$ (**a**), Me (**b**)). The complexes have been isolated from an unprecedented core conversion reaction of $Ru_2Cl(O_2CR)_4$ with 1-methylimidazole in methanol. The complexes display a $[Ru_2(\mu-L)(\eta^1:\mu-O_2CR)(\eta^1:\eta^1:\mu-O_2CR)_2]^{2+}$ ($L = OMe$ or η^1-O_2CR) core having the shortest Ru—Ru distance among d^5-d^5 ESBO complexes.^{5–10} Interestingly, the Ru—Ru single bond distance falls within the range 2.471–2.501 Å observed^{1,11} for d^2-d^2 and d^3-d^3 alkoxide-bridged ESBO complexes having a formal M—M double

- [†]Dedicated to Professor F. A. Cotton on the occasion of his 65th birthday.
- [‡]Abstract published in *Advance ACS Abstracts*, September 1, 1994.
- (1) Cotton, F. A. *Polyhedron* 1987, 6, 667.
- (2) Shaik, S.; Hoffmann, R.; Fisel, C. R.; Summerville, R. H. *J. Am. Chem. Soc.* 1980, 102, 4555.
- (3) Cotton, F. A.; Walton, R. A. *Multiple Bonds Between Metal Atoms*; Wiley-Interscience: New York, 1982.
- (4) (a) Cotton, F. A.; Su, J.; Sun, Z.-S.; Chen, H. *Inorg. Chem.* 1993, 32, 4871. (b) Poli, R.; Torralba, R. C. *Inorg. Chim. Acta* 1993, 212, 123. (c) Cotton, F. A.; Eglin, J. L.; James, C. A.; Luck, R. L. *Inorg. Chem.* 1992, 31, 5308. (d) Poli, R.; Mui, H. D. *Inorg. Chem.* 1991, 30, 65. (e) Cotton, F. A.; Shang, M.; Wojtezak, W. A. *Inorg. Chem.* 1991, 30, 3670. (f) Shaikh, S. N.; Zubietta, J. *Inorg. Chem.* 1988, 27, 1896. (g) Agaskar, P. A.; Cotton, F. A.; Dunbar, K. R.; Falvello, L. R.; O'Connor, C. J. *Inorg. Chem.* 1987, 26, 4051. (h) Kang, H.; Lui, S.; Shaikh, S. N.; Nicholson, T.; Zubietta, J. *Inorg. Chem.* 1989, 28, 920. (i) Winter, C. H.; Sheridan, P. H.; Heeg, M. J. *Inorg. Chem.* 1991, 30, 1962. (j) Cotton, F. A.; Daniels, L. M.; Dunbar, K. M.; Falvello, L. R.; O'Connor, C. J.; Price, A. C. *Inorg. Chem.* 1991, 30, 2509. (k) Chisholm, M. H.; Johnston, V. J.; Streib, W. E. *Inorg. Chem.* 1992, 31, 4081. (l) Danopoulos, A. A.; Wilkinson, G.; Hussain-Bates, B.; Hursthouse, M. B. *J. Chem. Soc., Dalton Trans.* 1990, 2753. (m) Clegg, W.; Errington, R. J.; Redshaw, C. J. *Chem. Soc., Dalton Trans.* 1992, 3189. (n) Yan, Y. K.; Chan, H. S. O.; Hor, T. S. A.; Tan, K.-L.; Lui, L.-K.; Wen, Y.-S. *J. Chem. Soc., Dalton Trans.* 1992, 423. (o) Redshaw, C.; Wilkinson, G.; Hussain-Bates, B.; Hursthouse, M. B. *J. Chem. Soc., Dalton Trans.* 1992, 555. (p) Clegg, W.; Errington, R. J.; Krazner, P.; Redshaw, C. J. *Chem. Soc., Dalton Trans.* 1992, 1431. (q) Clegg, W.; Errington, R. J.; Flynn, R. J.; Green, M. E.; Hockless, D. C. R.; Norman, N. C.; Gibson, V. C.; Tavakkoli, K. *J. Chem. Soc., Dalton Trans.* 1992, 1753. (r) Chen, X.-T.; Kang, B.-S.; Hu, Y.-H.; Xu, Y.-J. *J. Coord. Chem.* 1993, 30, 71. (s) Chang, Y.; Chen, Q.; Khan, M. I.; Salta, J.; Zubietta, J. *J. Chem. Soc., Chem. Commun.* 1993, 1872. (t) Bradley, D. C.; Chudzynska, H.; Hursthouse, M. B.; Motevali, M.; Wu, R. *Polyhedron* 1994, 13, 1. (u) Power, J. M.; Evertz, K.; Henling, L.; Mash, R.; Schaefer, W. P.; Labinger, J. A.; Bercaw, J. E. *Inorg. Chem.* 1990, 29, 5058.
- (5) Cotton, F. A.; Matusz, M.; Torralba, R. C. *Inorg. Chem.* 1989, 28, 1516.
- (6) Chakravarty, A. R.; Cotton, F. A.; Diebold, M. P.; Lewis, D. B.; Roth, W. J. *J. Am. Chem. Soc.* 1986, 108, 971.

(7) Flood, M. T.; Ziolo, R. J.; Earley, J. F.; Gray, H. B. *Inorg. Chem.* 1973, 12, 2153.

(8) Chakravarty, A. R.; Cotton, F. A.; Tocher, D. A. *Inorg. Chem.* 1984, 23, 4030.

bond. Complexes **1** and **2** with a $\sigma^2\pi^2\delta^2\delta^*\pi^{*2}$ electronic configuration exhibit reversible redox chemistry involving π^* and σ^* molecular orbitals, and this work provides electrochemical evidence for the mixed-valence type **II** diruthenium ESBO cores.

Experimental Section

The preparative procedure for $\text{Ru}_2\text{Cl}(\text{O}_2\text{CR})_4$ ($\text{R} = \text{C}_6\text{H}_4-p\text{-X}; \text{X} = \text{OMe, Me}$) was reported¹² earlier. 1-Methylimidazole (1-MeIm) was from Fluka.

Preparations. The complexes $[\text{Ru}_2(\text{OMe})(\text{O}_2\text{CC}_6\text{H}_4-p\text{-X})_3(1\text{-MeIm})_4](\text{ClO}_4)_2$ ($\text{X} = \text{OMe}$ (**1a**), Me (**1b**)) and $[\text{Ru}_2(\text{O}_2\text{CC}_6\text{H}_4-p\text{-X})_4(1\text{-MeIm})_4](\text{ClO}_4)_2$ ($\text{X} = \text{OMe}$ (**2a**), Me (**2b**)) were prepared using a general procedure in which 200 mg of $\text{Ru}_2\text{Cl}(\text{O}_2\text{CR})_4$ (1.0 mmol) in 10 mL of methanol was reacted with 2 mL of 1 mM solution of 1-MeIm in MeOH under stirring conditions for 30 min at 10 °C. The resulting brown solution was filtered, and the filtrate was treated with NaClO₄. A crude yellow solid was precipitated with diethyl ether in ~75% yield. The product was subjected to chromatography on a silica gel column in CHCl₃. A yellow band containing **2** was eluted first using a 19:1 v/v mixture of CHCl₃–MeOH as eluant. A greenish-yellow band containing **1** was eluted next from the column using a 9:1 v/v mixture of CHCl₃–MeOH. The crude product decomposed partially on the silica gel surface. The yield of the complexes ranged between 20 and 30%. Complex **2** was also prepared in ~40% yield by treating $\text{Ru}_2\text{Cl}(\text{O}_2\text{CR})_4$ with 1-methylimidazole in a 1:8 mole ratio in ethanol (10 mL) followed by precipitation of the complex as a perchlorate salt. The formation of any ethoxy species was not observed from this reaction which gave $[\text{Ru}_2\text{O}(\text{O}_2\text{CR})_2(1\text{-MeIm})_6](\text{ClO}_4)_2$ ¹³ as the other product in 50% yield. Anal. Calcd for **1a**, $\text{C}_{41}\text{H}_{48}\text{N}_8\text{O}_{18}\text{Cl}_2\text{Ru}_2$: C, 40.55; H, 3.96; N, 9.23. Found: C, 40.65; H, 4.03; N, 9.38. Calcd for **1b**, $\text{C}_{41}\text{H}_{48}\text{N}_8\text{O}_{15}\text{Cl}_2\text{Ru}_2$: C, 42.22; H, 4.12; N, 9.61. Found: C, 42.33; H, 4.51; N, 9.82. Calcd for **2a**, $\text{C}_{48}\text{H}_{52}\text{N}_8\text{O}_{20}\text{Cl}_2\text{Ru}_2$: C, 43.20; H, 3.93; N, 8.40. Found: C, 43.69; H, 4.08; N, 8.85. Calcd for **2b**, $\text{C}_{48}\text{H}_{52}\text{N}_8\text{O}_{16}\text{Cl}_2\text{Ru}_2$: C, 45.37; H, 4.10; N, 8.82. Found: C, 44.87; H, 4.53; N, 8.63. The complexes are soluble in polar organic solvents and are moderately stable in solution. The hexafluoro salt of **1a**, $[\text{Ru}_2(\text{OMe})(\text{O}_2\text{CC}_6\text{H}_4-p\text{-OMe})_3(1\text{-MeIm})_4](\text{PF}_6)_2$ (**1a'**), was prepared by treating **1a** with $[\text{Bu}^n\text{N}](\text{PF}_6)$ in MeCN followed by precipitation with diethyl ether. Anal. Calcd for **1a'**, $\text{C}_{41}\text{H}_{48}\text{N}_8\text{O}_{10}\text{F}_{12}\text{P}_2\text{Ru}_2$: C, 37.72; H, 3.68; N, 8.59. Found: C, 37.45; H, 3.99; N, 8.13.

Caution! Perchlorate salts are potentially explosive and should be handled carefully in small quantities under appropriate safety conditions.

Measurements. The elemental analysis was done with a Heraeus CHN-O Rapid instrument. The ¹H NMR spectra were recorded with Bruker ACF 200 MHz and WH 270 MHz spectrometers. Conductivity measurements were done with a Century CC603 conductivity meter. Cyclic and differential pulse voltammetric measurements were made at 25 °C using a three-electrode setup comprising a platinum button working, a platinum wire auxiliary electrode, and a saturated calomel reference electrode on a PAR Model 174A polarographic analyzer

- (9) (a) Chakravarty, A. R.; Cotton, F. A. *Inorg. Chem.* **1985**, *24*, 3584.
(b) Chakravarty, A. R.; Cotton, F. A.; Tocher, D. A. *J. Am. Chem. Soc.* **1984**, *106*, 6409.
- (10) Kelson, E. P.; Henling, L. M.; Schaefer, W. P.; Labinger, J. A.; Bercaw, J. E. *Inorg. Chem.* **1993**, *32*, 2863.
- (11) (a) Cotton, F. A.; Diebold, M. P.; Roth, W. *Inorg. Chem.* **1985**, *24*, 3509. (b) Chisholm, M. H.; Kirkpatrick, C. C.; Huffmann, J. C. *Inorg. Chem.* **1981**, *20*, 871. (c) Cotton, F. A.; DeMarco, D.; Kolthammer, B. W. S.; Walton, R. A. *Inorg. Chem.* **1981**, *20*, 3048. (d) Barder, T. J.; Cotton, F. A.; Lewis, D.; Schwotzer, W.; Tetrick, S. M.; Walton, R. A. *J. Am. Chem. Soc.* **1984**, *106*, 2882. (e) Anderson, L. B.; Cotton, F. A.; DeMarco, D.; Falvello, L. R.; Tetrick, S. M.; Walton, R. A. *J. Am. Chem. Soc.* **1984**, *106*, 4743. (f) Anderson, L. B.; Cotton, F. A.; DeMarco, D.; Fang, A.; Ilsley, W. H.; Kolthammer, B. W. S.; Walton, R. A. *J. Am. Chem. Soc.* **1981**, *103*, 5078. (g) Cotton, F. A.; DeMarco, D.; Falvello, L. R.; Walton, R. A. *J. Am. Chem. Soc.* **1983**, *105*, 3088. (h) Chisholm, M. H.; Corning, J. F.; Folting, K.; Huffmann, J. C.; Ratermann, A. L.; Rothwell, I. P.; Streib, W. E. *Inorg. Chem.* **1984**, *23*, 1037.
- (12) Das, B. K.; Chakravarty, A. R. *Polyhedron* **1988**, *7*, 685.
- (13) Sudha, C.; Mandal, S. K.; Chakravarty, A. R. *Inorg. Chem.* **1993**, *32*, 3801.

Table 1. Crystallographic Data for $[\text{Ru}_2(\text{OMe})(\text{O}_2\text{CC}_6\text{H}_4-p\text{-OMe})_3(1\text{-MeIm})_4](\text{PF}_6)_2 \cdot 1.5\text{MeCN} \cdot 0.5\text{Et}_2\text{O}$ (**1a'**·1.5MeCN·0.5Et₂O) and $[\text{Ru}_2(\text{O}_2\text{CC}_6\text{H}_4-p\text{-OMe})_4(1\text{-MeIm})_4](\text{ClO}_4)_2$ (**2a**)

chem formula	$\text{C}_{46}\text{H}_{57}\text{N}_{9.5}\text{O}_{10.5}\text{F}_{12}\text{P}_2\text{Ru}_2$	$\text{C}_{48}\text{H}_{52}\text{N}_8\text{O}_{20}\text{Cl}_2\text{Ru}_2$
fw	1403.59	1334.03
<i>a</i> , Å	13.125(2)	8.950(1)
<i>b</i> , Å	15.529(3)	12.089(3)
<i>c</i> , Å	17.314(5)	13.735(3)
α , deg	67.03(2)	81.09(2)
β , deg	68.05(2)	72.27(1)
γ , deg	81.38(1)	83.15(2)
<i>V</i> , Å ³	3014(1)	1394(1)
<i>Z</i>	2	1
space group	$P\bar{1}$ (No. 2)	$P\bar{1}$ (No. 2)
<i>T</i> , °C	18	18
λ , Å	0.7107	0.7107
Q_{calcd} , g cm ⁻³	1.55	1.59
μ , cm ⁻¹	6.37	7.05
$R(F_o)^a$	0.0607	0.0549
$R_w(F_o)^b$	0.0627	0.0534
<i>g</i>	0.000 926	0.000 147

$$^a R(F_o) = (\sum |F_o| - |F_c|)/(\sum |F_o|). \quad ^b R_w(F_o) = [(\sum w^{1/2} |F_o| - |F_c|)/(\sum w^{1/2} |F_o|)]; w = [\sigma^2(F_o) + gF_o^2]^{-1}.$$

connected to a drop timer and a Houston Instruments Omnidigraphic X-Y recorder. For the differential pulse voltammetric experiments, the pulse amplitude and drop time were 50 mV (p–p) and 0.5 s, respectively. The electrochemical data are uncorrected for junction potentials. Ferrocene was used as an internal standard to determine the electron transfer stoichiometries from the cathodic and anodic peak current measurements. The nature of the electron transfer was determined by electrolysis done at a potential 200 mV higher than the anodic peak potential (E_{pa}) and 200 mV lower than the cathodic peak potential (E_{pc}). The reversibility of the process was determined from the peak to peak separations (ΔE_p) of the cyclic voltammograms at various scan rates and from the width at half-height (δ) of the differential pulse voltammograms. The i_{pc}/i_{pa} and I_{bs}/I_{fs} ratios at various scan rates were also used to determine the reversibility of the process, where i_{pc} and i_{pa} are the cathodic and anodic peak currents of the cyclic voltammograms and I_{bs} and I_{fs} are the backward-scan and forward-scan peak currents of the differential pulse voltammograms, respectively.

X-ray Crystallography. Pale greenish-yellow rectangular shaped crystals of **1a'** were obtained on cooling a solution of the complex in an acetonitrile–diethyl ether mixture. A crystal of approximate size $0.33 \times 0.14 \times 0.09$ mm³ was fixed inside a Lindemann capillary along with the mother liquor. The unit cell parameters were obtained from this crystal mounted on an Enraf-Nonius CAD4 diffractometer using graphite-monochromated Mo K α radiation. Intensity data, collected in the 2θ range 2–50° by the $\omega - 2\theta$ scan technique for $+h$, $\pm k$, $\pm l$ reflections in the triclinic crystal system, were corrected for Lorentz, polarization, and absorption¹⁴ effects (transmission coefficient: 0.80–0.98). Yellow rectangular crystals of **2a** were obtained from slow evaporation of a solution of the complex in MeCN–H₂O at 5 °C. A crystal of approximate size $0.2 \times 0.08 \times 0.06$ mm³ was mounted on a glass fiber. The unit cell parameters were obtained similarly to those for **1a'**. The data collection and reduction procedures for the triclinic crystal of **2a** were the same as those for **1a'** (transmission coefficient: 0.82–0.98).

The structures of **1a'** and **2a** were solved in the space group $P\bar{1}$ by the heavy-atom method and Fourier synthesis using the SHELX system of programs¹⁵ on a VAX-8810 computer. The atom scattering factors were taken from ref 16. There were 10 601 data for **1a'**, of which 4672 with $I > 2.5\sigma(I)$ were used for structure solution and refinement.

- (14) North, A. C. T.; Phillips, D. C.; Mathews, F. S. *Acta Crystallogr.* **1968**, *A24*, 351.
- (15) (a) Sheldrick, G. M. *SHELX76: A Program for Crystal Structure Determination*; University of Cambridge: Cambridge, England, 1976.
(b) Sheldrick, G. M. *SHELXS-86: A Program for Crystal Structure Solution*; Universität Göttingen: Göttingen, Germany, 1986.
- (16) *International Tables for X-ray Crystallography*; Kynoch Press: Birmingham, England, 1974; Vol. 4.

Table 2. ^1H NMR Spectral and Electrochemical Data^a for $[\text{Ru}_2(\text{OMe})(\text{O}_2\text{CC}_6\text{H}_4-p-\text{X})_3(1\text{-MeIm})_4](\text{ClO}_4)_2$ ($\text{X} = \text{OMe}$ (**1a**), Me (**1b**)) and $[\text{Ru}_2(\text{O}_2\text{CC}_6\text{H}_4-p-\text{X})_4(1\text{-MeIm})_4](\text{ClO}_4)_2$ ($\text{X} = \text{OMe}$ (**2a**), Me (**2b**))

complex	^1H NMR (CD_3CN): δ , ppm [πH]			
	$\text{Me}(\text{O}_2\text{CR})$	1-MeIm	OMe	$\text{O}_2\text{CC}_6\text{H}_4-p-\text{X}, 1\text{-MeIm}$
1a	3.76 [3H], 3.84 [6H]	3.68 [6H], 3.93 [6H]	3.29 [3H]	6.6–8.2 [24H]
1b	2.28 [3H], 2.38 [6H]	3.67 [6H], 3.93 [6H]	3.31 [3H]	6.9–8.2 [24H]
2a	3.77 [6H], 3.87 [6H]	3.68 [12H]		6.6–8.2 [28H]
2b	2.28 [6H], 2.40 [6H]	3.64 [12H]		6.9–8.2 [28H]

Cyclic Voltammetry: $E_{1/2}$, V vs SCE (ΔE_p , mV at 20 mV s ⁻¹)						
complex	couple			couple		
	Ru ^{III} , Ru ^{III} /Ru ^{III} , Ru ^{IV}	Ru ^{III} , Ru ^{III} /Ru ^{III} , Ru ^{II}	complex	Ru ^{III} , Ru ^{III} /Ru ^{III} , Ru ^{IV}	Ru ^{III} , Ru ^{III} /Ru ^{III} , Ru ^{II}	
1a	1.58 (65)	−0.41 (60)	2a	1.64 ^b		−0.09 (60)
1b	1.64 (65)	−0.39 (60)	2b	1.70 ^b		−0.03 (65)

Differential Pulse Voltammetry: E_{fs} , V vs SCE (δ , mV at 2 mV s ⁻¹ ; I_{bs}/I_{fs})						
complex	couple			couple		
	Ru ^{III} , Ru ^{III} /Ru ^{III} , Ru ^{IV}	Ru ^{III} , Ru ^{III} /Ru ^{III} , Ru ^{II}	complex	Ru ^{III} , Ru ^{III} /Ru ^{III} , Ru ^{IV}	Ru ^{III} , Ru ^{III} /Ru ^{III} , Ru ^{II}	
1a	1.53 (95; 1.0)	−0.40 (90; 0.5)	2a	1.56 (120; 0.5)		−0.07 (90; 0.5)
1b	1.59 (95; 1.0)	−0.38 (90; 0.6)	2b	1.60 (120; 0.7)		−0.04 (90; 0.5)

^a In MeCN–0.1 M TBAP. $E_{1/2} = (E_{pa} + E_{pc})/2$; $\Delta E_p = E_{pa} - E_{pc}$; δ = peak width at half-height; E_{pa} , E_{pc} , and E_{fs} are peak anodic, peak cathodic, and forward-scan peak potentials, respectively. I_{bs} and I_{fs} are backward-scan and forward-scan peak currents, respectively. ^b The anodic response (E_{pa}) without any well-resolved cathodic counterpart.

Table 3. Positional Parameters and Isotropic Thermal Parameters ($\times 10^3$) for Non-Hydrogen Atoms in **1a**·1.5MeCN·0.5Et₂O

atom	<i>x</i>	<i>y</i>	<i>z</i>	$U_{eq(iso)}$, Å ²	atom	<i>x</i>	<i>y</i>	<i>z</i>	$U_{eq(iso)}$, Å ²
Ru1	0.3149(1)	1.0936(1)	0.6921(1)	33(1)	C29	0.1807(16)	1.4508(12)	0.5306(13)	117(13)
Ru2	0.2304(1)	0.9354(1)	0.7758(1)	33(1)	N3	0.4687(8)	1.1476(6)	0.6224(6)	45(5)
O1	0.3909(6)	0.9679(5)	0.7156(5)	36(4)	C31	0.5232(12)	1.1871(10)	0.5339(9)	64(7)
O2	0.2141(7)	0.9451(5)	0.6589(5)	42(4)	C32	0.6203(12)	1.2246(11)	0.5152(10)	76(9)
O3	0.2935(6)	1.0901(5)	0.5806(5)	38(4)	N4	0.6233(9)	1.2091(7)	0.5974(8)	59(6)
O4	0.2546(7)	0.9375(5)	0.8845(5)	42(4)	C30	0.5306(11)	1.1640(9)	0.6615(8)	51(6)
O5	0.3272(7)	1.0825(6)	0.8111(5)	46(5)	C33	0.7101(13)	1.2423(11)	0.6121(12)	91(10)
O6	0.1514(6)	1.0601(5)	0.7505(5)	36(4)	N5	0.2870(7)	0.8007(6)	0.8033(6)	40(5)
O7	0.0781(8)	1.0764(6)	0.8846(5)	59(5)	N6	0.3154(9)	0.6583(7)	0.8034(9)	70(7)
C1	0.4621(11)	0.9394(8)	0.6420(8)	49(7)	C34	0.2778(10)	0.7431(8)	0.7655(9)	54(7)
C2	0.2400(9)	1.0206(9)	0.5911(8)	41(6)	C35	0.3311(11)	0.7501(8)	0.8669(8)	53(7)
C3	0.2096(9)	1.0294(8)	0.5125(7)	34(6)	C36	0.3487(12)	0.6615(10)	0.8681(10)	74(9)
C4	0.1587(11)	0.9565(9)	0.5136(8)	52(8)	C37	0.3245(16)	0.5777(11)	0.7751(15)	118(14)
C5	0.1327(11)	0.9662(10)	0.4402(9)	55(8)	N7	0.0787(7)	0.8765(7)	0.8511(6)	45(5)
C6	0.1534(10)	1.0511(8)	0.3663(8)	44(6)	C39	0.0139(10)	0.8752(8)	0.9374(7)	47(6)
C7	0.1979(12)	1.1241(9)	0.3671(9)	60(7)	C40	−0.0750(12)	0.8277(10)	0.9596(9)	67(8)
C8	0.2266(11)	1.1145(8)	0.4382(9)	54(7)	N8	−0.0703(9)	0.7978(7)	0.8955(7)	56(6)
O8	0.1285(8)	1.0661(6)	0.2928(6)	65(5)	C38	0.0240(10)	0.8313(8)	0.8294(8)	44(6)
C9	0.0888(11)	0.9904(9)	0.2846(9)	61(8)	C41	−0.1535(11)	0.7445(10)	0.8930(10)	76(9)
C10	0.2980(10)	1.0077(9)	0.8804(8)	40(6)	P1	0.9472(4)	0.3478(3)	0.3428(4)	87(3)
C11	0.3178(10)	1.0034(8)	0.9608(8)	43(6)	F11	0.9501(15)	0.2689(14)	0.4230(10)	235(14)
C12	0.2995(11)	0.9206(10)	1.0331(8)	57(7)	F12	0.8274(10)	0.3763(11)	0.3908(11)	209(12)
C13	0.3166(13)	0.9158(10)	1.1093(9)	66(8)	F13	1.0638(10)	0.3287(10)	0.2928(9)	192(10)
C14	0.3580(10)	0.9955(10)	1.1085(8)	50(7)	F14	0.8968(18)	0.2805(13)	0.3281(16)	269(21)
C15	0.3808(11)	1.0756(8)	1.0350(8)	48(7)	F15	0.9413(16)	0.4272(20)	0.2668(12)	414(19)
C16	0.3602(10)	1.0788(8)	0.9619(8)	44(7)	F16	0.9881(17)	0.4058(18)	0.3697(25)	370(32)
O9	0.3770(8)	0.9805(6)	1.1851(5)	61(5)	P2	0.4834(5)	0.3579(4)	0.9418(4)	107(4)
C17	0.4123(11)	1.0590(11)	1.1909(9)	67(9)	F21	0.4023(16)	0.3188(11)	0.9194(11)	205(13)
C18	0.0781(10)	1.1012(8)	0.8108(8)	42(7)	F22	0.4521(12)	0.2759(8)	1.0356(8)	167(9)
C19	0.0117(10)	1.1753(8)	0.7690(7)	42(6)	F23	0.5100(9)	0.4387(7)	0.8494(8)	150(8)
C20	0.0167(10)	1.2026(8)	0.6808(8)	50(7)	F24	0.5712(19)	0.3915(12)	0.9582(14)	298(19)
C21	−0.0462(12)	1.2782(10)	0.6448(9)	65(8)	F25	0.3927(17)	0.4184(12)	0.9763(11)	268(14)
C22	−0.1152(11)	1.3232(9)	0.6997(11)	63(9)	F26	0.5589(17)	0.2927(10)	0.8963(11)	248(14)
C23	−0.1230(10)	1.2982(9)	0.7878(9)	61(7)	C42	0.3502(20)	0.3680(19)	0.1958(15)	135(17)
C24	−0.0591(12)	1.2244(10)	0.8199(9)	64(8)	C43	0.3755(22)	0.3413(17)	0.2703(22)	147(20)
O10	−0.1717(9)	1.3972(7)	0.6556(7)	92(7)	N9	0.3921(22)	0.3164(16)	0.3426(15)	153(16)
C25	−0.2368(17)	1.4517(14)	0.7059(12)	127(12)	O11	0.4769(36)	0.5330(28)	0.4638(28)	324(21) ^b
N1	0.2665(8)	1.2302(6)	0.6664(6)	40(5)	C44	0.5264(41)	0.5342(32)	0.3875(34)	303(24) ^b
C26	0.2502(11)	1.2900(9)	0.5907(9)	55(7)	C45	0.5092(41)	0.5973(36)	0.3133(34)	160(19) ^b
C27	0.2372(12)	1.2799(9)	0.7214(8)	58(8)	C46	1.0000	0.5000	1.0000	197(18) ^b
N2	0.2119(10)	1.3707(7)	0.5981(8)	67(7)	C47	0.9567(50)	0.4519(43)	0.9728(42)	178(25) ^b
C28	0.1994(13)	1.3663(9)	0.6808(11)	73(8)	N10	0.9219(43)	0.4248(36)	0.9484(35)	195(22) ^b

^a The expression for the equivalent isotropic thermal parameter is $U_{eq} = (\sum_i \sum_j U_{ij} a_i^* a_j^* a_i a_j)/3$. ^b Atoms were refined isotropically with a site occupancy factor of 0.5.

The hydrogen atoms belonging to the complex cation were used only for structure factor calculations with a fixed isotropic equivalent thermal parameter of 0.10 Å². The asymmetric unit of the cell showed the presence of solvent molecules besides a complex cation and two PF₆ anions. One MeCN molecule refined well with a site occupancy of

1.0. However, another molecule was located near the edge of the cell with one atom at a special position on the edge with a site occupancy factor of 0.5. This molecule was modeled as a 2-fold-disordered MeCN, thus giving a 0.5 MeCN for the asymmetric unit. The difference Fourier map showed three additional peaks giving a p–p–p (p = peak) angle

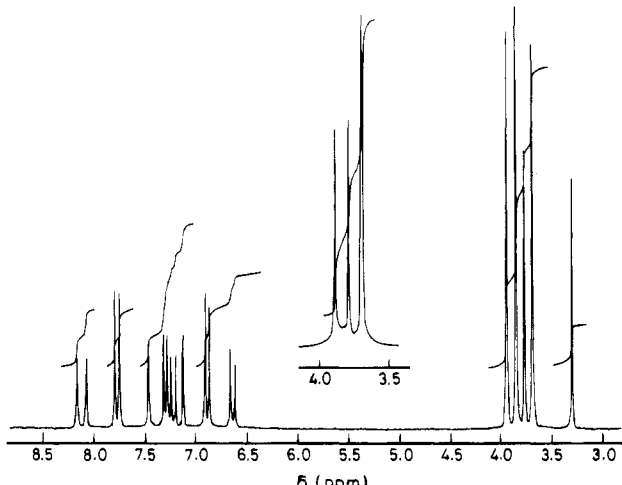


Figure 1. ^1H NMR spectrum of $[\text{Ru}_2(\text{OMe})(\text{O}_2\text{CC}_6\text{H}_4\text{-}p\text{-OMe})_3(1\text{-MeIm})_4](\text{ClO}_4)_2$ (**1a**) in CD_3CN . The inset shows the methyl signals of $[\text{Ru}_2(\text{O}_2\text{CC}_6\text{H}_4\text{-}p\text{-OMe})_4(1\text{-MeIm})_4](\text{ClO}_4)_2$ (**2a**).

of 125° . These peaks generated three inversion-symmetry-related centers showing a short contact of 1.5 \AA . The modeling of these peaks for MeCN was not attempted since the p–p–p angle deviated greatly from 180° . The peaks were, however, assigned to a diethyl ether molecule. The whole structure refined well as $[\text{Ru}_2(\text{OMe})(\text{O}_2\text{CC}_6\text{H}_4\text{-}p\text{-OMe})_3(1\text{-MeIm})_4](\text{PF}_6)_2\cdot 1.5 \text{ MeCN}\cdot 0.5 \text{ Et}_2\text{O}$ (**1a'** \cdot $1.5 \text{ MeCN}\cdot 0.5 \text{ Et}_2\text{O}$). The final difference Fourier map was featureless, showing the highest peak of $0.82 \text{ e}/\text{\AA}^3$ near Ru1. The overall scale factor was 1.0 for the highest shift/esd of 0.10 in the final full-matrix least-squares refinement cycle using 724 parameters.

For the structure solution and refinement of **2a**, 3004 reflections with $I > 2.5\sigma(I)$ were used. The hydrogen atoms located in the Fourier maps were used only for structure factor calculations with an isotropic equivalent thermal parameter of 0.1 \AA^2 . All other atoms were refined anisotropically. The final difference Fourier map showed the highest peak of $0.88 \text{ e}/\text{\AA}^3$ near Ru1. The overall scale factor was 1.42 for the highest shift/esd of -0.1 in the final full-matrix least-squares refinement cycle involving 361 parameters. Selected crystallographic data for **1a'** \cdot $1.5 \text{ MeCN}\cdot 0.5 \text{ Et}_2\text{O}$ and **2a** are presented in Table 1.

Results and Discussion

Synthetic and Spectral Aspects. Tetracarboxylates with a “paddle-wheel” structure are useful precursors for the synthesis of other types of multiply bonded systems.^{3,17} Among these precursors, the diruthenium species is unique because of the unusual stability of the Ru_2^{5+} mixed-valence state.¹⁸ While unidentate O- and N-donor ligands are capable of substituting the axial and/or equatorial ligands of the tetracarboxylate framework of Cr_2 , Mo_2 , Rh_2 , and Re_2 systems, similar reactions with $\text{Ru}_2\text{Cl}(\text{O}_2\text{CR})_4$ effect a core conversion, forming tribridged (μ -oxo)bis(μ -carboxylato)diruthenium(III) complexes.^{13,19}

The reaction of $\text{Ru}_2\text{Cl}(\text{O}_2\text{CR})_4$ with 1-methylimidazole (**1-MeIm**) in methanol leads to the formation of two unusual types of ESBO diruthenium(III) complexes, $[\text{Ru}_2(\text{OMe})(\text{O}_2\text{CR})_3(1\text{-MeIm})_4]^{2+}$ and $[\text{Ru}_2(\text{O}_2\text{CR})_4(1\text{-MeIm})_4]^{2+}$, isolated as perchlorate salts. The complexes are 1:2 electrolytes showing a Λ_M value of $230 \text{ mhos cm}^2 \text{ M}^{-1}$ in MeCN. The electronic spectra of the yellow solutions of the complexes in acetonitrile display

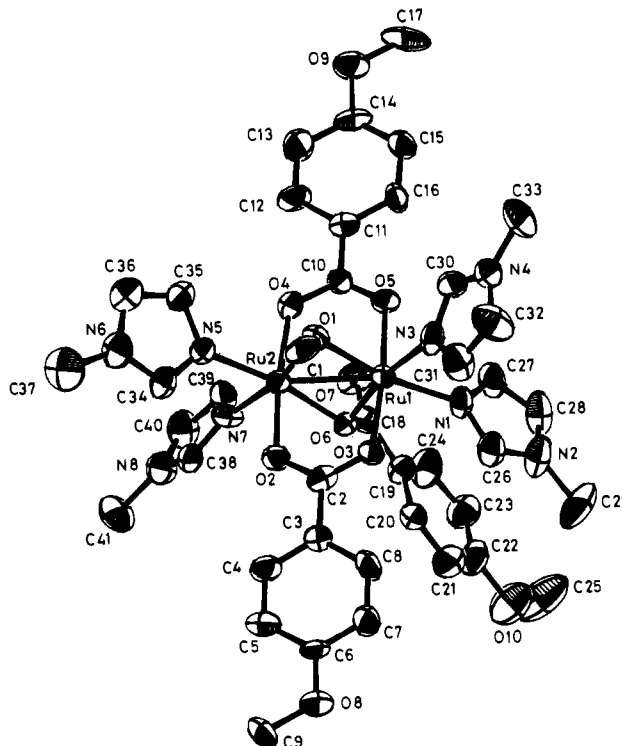


Figure 2. ORTEP drawing of the cationic complex in $[\text{Ru}_2(\text{OMe})(\text{O}_2\text{CC}_6\text{H}_4\text{-}p\text{-OMe})_3(1\text{-MeIm})_4](\text{PF}_6)_2\cdot 1.5 \text{ MeCN}\cdot 0.5 \text{ Et}_2\text{O}$ with atom-numbering scheme.

a shoulder at 350 nm . The ^1H NMR spectral data for **1** and **2** are given in Table 2. The ^1H NMR spectra of **1a** and **1b** display five methyl signals (Figure 1), indicating the presence of two chemically inequivalent RCO_2^- and 1-MeIm ligands. The methyl peaks are assigned to ligands in a 1:1:2:2:2 OMe: RCO_2^- : RCO_2^- :1-MeIm:1-MeIm ratio. The tetracarboxylate-bridged complexes **2a** and **2b** show only three methyl signals in a 1:1:2 RCO_2^- : RCO_2^- :1-MeIm ratio (Figure 1). The true nature of the complexes is obtained from the X-ray diffraction studies.

X-ray Structures. To understand the structure and bonding of the ESBO complexes, the crystal structures of **1a'** and **2a** have been determined. ORTEP²⁰ views of the cationic complexes in **1a'** \cdot $1.5 \text{ MeCN}\cdot 0.5 \text{ Et}_2\text{O}$ and **2a** are shown in Figures 2 and 3, respectively. The atomic positional parameters of the complexes are given in Tables 3 and 4, selected bond distances and angles are listed in Tables 5 and 6.

The structures consist of a diruthenium unit held by two three-atom and two monoatomic bridging ligands. The overall structure of the molecule is a type II ESBO with a N_2O_4 octahedral geometry around the metal centers. The 1-MeIm ligands occupy the terminal sites (L_t) of the core. The presence of monoatomic methoxy and carboxylate bridges in **1a'** makes it a rare example of an asymmetrically bridged ESBO structure.

The unprecedented type of conversion of a $\text{Ru}_2(\eta^1:\eta^1:\mu\text{-O}_2\text{CR})_4^+$ unit with a metal–metal bond order of 2.5 to a $\text{Ru}_2(\eta^1:\mu\text{-O}_2\text{CR})_2(\eta^1:\eta^1:\mu\text{-O}_2\text{CR})_2^{2+}$ core having a Ru–Ru single bond in **2** involves a one-electron oxidation of the precursor core, the loss of one chloride, and an intramolecular shift of two carboxylate ligands from a three-atom to a monoatomic bridging mode. The formation of **1** presumably arises from the substitution of one monoatomic bridging carboxylate ligand in **2** by a methoxy ligand from methanol solvent.²¹ However, a similar

(17) Cotton, F. A.; Walton, R. A. *Struct. Bonding (Berlin)* **1985**, 62, 1.
(18) Norman, J. G., Jr.; Renzoni, G. E.; Case, D. A. *J. Am. Chem. Soc.* **1979**, 101, 5256.

(19) (a) Mitchell, R. W.; Spencer, A.; Wilkinson, G. *J. Chem. Soc., Dalton Trans.* **1973**, 846. (b) Das, B. K.; Chakravarty, A. R. *Inorg. Chem.* **1991**, 30, 4978. (c) Das, B. K.; Chakravarty, A. R. *Inorg. Chem.* **1990**, 29, 2078. (d) Barral, M. C.; Jimenez-Aparicio, R.; Royer, E. C.; Urbanos, F. A.; Monge, A.; Ruizvalero, C. *Polyhedron* **1991**, 10, 113. (e) Barral, M. C.; Jimenez-Aparicio, R.; Kramolowsky, R.; Wagner, I. *Polyhedron* **1993**, 12, 903.

(20) Johnson, C. K. ORTEP. Report ORNL-3794; Oak Ridge National Laboratory: Oak Ridge, TN, 1971.

(21) Mandal, S. K.; Chakravarty, A. R. *Inorg. Chim. Acta* **1987**, 132, 157.

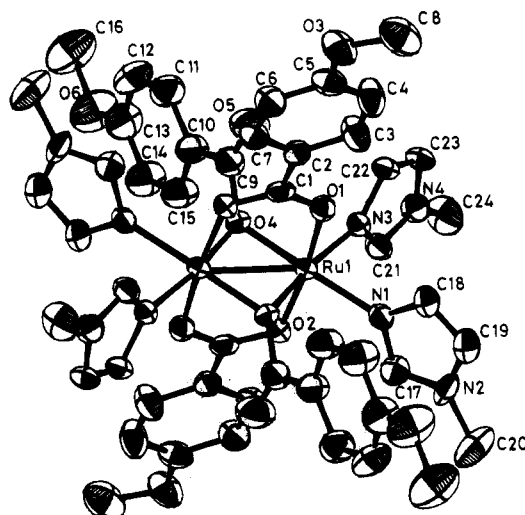


Figure 3. ORTEP view of the cationic complex in $[\text{Ru}_2(\text{O}_2\text{CC}_6\text{H}_4-p\text{-OMe})_4(1\text{-MeIm})_4](\text{ClO}_4)_2$ (**2a**) with atom-labeling scheme.

Table 4. Positional Parameters and Isotropic Thermal Parameters ($\times 10^3$) for Non-Hydrogen Atoms in **2a**

atom	<i>x</i>	<i>y</i>	<i>z</i>	$U_{\text{eq(iso)}} \text{ \AA}^2$
Ru1	0.0331(1)	0.5926(1)	0.5136(1)	29(1)
O1	0.2333(6)	0.5761(4)	0.3931(4)	36(2)
O2	-0.1764(6)	0.5927(4)	0.6311(4)	35(2)
C1	0.2602(9)	0.4907(7)	0.3445(6)	36(3)
C2	0.3973(10)	0.4904(7)	0.2517(6)	38(3)
C3	0.4961(12)	0.5767(8)	0.2223(8)	59(4)
C4	0.6248(12)	0.5757(8)	0.1358(8)	62(4)
C5	0.6531(10)	0.4919(8)	0.0752(7)	49(4)
C6	0.5541(11)	0.4053(8)	0.1027(7)	50(4)
C7	0.4288(10)	0.4031(7)	0.1915(7)	42(4)
O3	0.7752(7)	0.4832(6)	-0.0131(5)	61(3)
C8	0.8610(14)	0.5799(11)	-0.0540(9)	82(6)
O4	0.0693(6)	0.4416(4)	0.5906(4)	37(2)
O5	0.3288(8)	0.3887(6)	0.5421(6)	76(3)
C9	0.2032(12)	0.3823(8)	0.6040(8)	48(4)
C10	0.1718(11)	0.3085(8)	0.7028(8)	53(4)
C11	0.2882(13)	0.2233(9)	0.7211(8)	61(5)
C12	0.2626(15)	0.1546(9)	0.8146(9)	72(5)
C13	0.1220(14)	0.1718(9)	0.8929(9)	69(5)
C14	0.0043(14)	0.2520(10)	0.8795(8)	69(5)
C15	0.0289(12)	0.3205(9)	0.7839(8)	61(4)
O6	0.0917(11)	0.1127(7)	0.9875(6)	95(4)
C16	0.2105(19)	0.0289(12)	1.0106(10)	104(8)
N1	-0.0084(8)	0.7566(6)	0.4613(5)	36(3)
N2	-0.1299(10)	0.9225(5)	0.4447(6)	50(3)
C17	-0.1404(10)	0.8208(7)	0.4963(6)	43(4)
C18	0.0892(11)	0.8233(7)	0.3826(7)	51(4)
C19	0.0148(12)	0.9252(8)	0.3722(8)	58(4)
C20	-0.2533(16)	1.0141(9)	0.4611(9)	85(6)
N3	0.1480(8)	0.6505(5)	0.5997(5)	34(3)
C21	0.0799(10)	0.7013(7)	0.6834(7)	41(3)
C22	0.3089(9)	0.6551(7)	0.5795(7)	41(4)
N4	0.1881(9)	0.7359(6)	0.7163(5)	43(3)
C23	0.3319(10)	0.7077(7)	0.6526(7)	44(3)
C24	0.1596(13)	0.7922(9)	0.8086(8)	68(5)
C11	-0.3860(3)	0.9118(2)	0.7734(2)	67(1)
O7	-0.2332(9)	0.8565(6)	0.7561(7)	87(4)
O8	-0.3733(9)	1.0284(6)	0.7652(8)	110(5)
O9	-0.4855(11)	0.8726(8)	0.8721(7)	117(4)
O10	-0.4514(11)	0.8865(8)	0.6961(7)	110(5)

^a The expression for the equivalent isotropic thermal parameter is $U_{\text{eq}} = (\sum_i \sum_j U_{ij} a_i^* a_j^* a_i a_j)/3$.

reaction in an ethanolic medium forms **2** and a tribridged species.¹³

The Ru—Ru distance in **1a'** and **2a** is the shortest among those for known^{5–10} ESBO diruthenium(III) complexes (Table 7). It is a general observation¹ that smaller bridging ligands

Table 5. Selected Bond Distances (Å) and Angles (deg) for **1a'·1.5MeCN·0.5Et₂O**

Ru1—Ru2	2.490(2)	Ru2—O1	2.011(7)
Ru1—O1	2.018(7)	Ru2—O2	2.059(10)
Ru1—O3	2.074(10)	Ru2—O4	2.035(10)
Ru1—O5	2.065(10)	Ru2—O6	2.023(7)
Ru1—O6	2.049(7)	Ru2—N5	2.043(9)
Ru1—N1	2.042(9)	Ru2—N7	2.043(8)
Ru1—N3	2.032(9)	O6—C18	1.417(15)
O1—C1	1.456(15)	O7—C18	1.182(17)
O2—C2	1.271(12)	C18—C19	1.459(17)
O3—C2	1.292(17)		
C2—C3	1.508(21)		
O4—C10	1.270(18)		
O5—C10	1.280(13)		
C10—C11	1.484(22)		
Ru1—O1—Ru2	76.4(3)	O1—Ru2—N7	168.2(4)
Ru1—O6—Ru2	75.4(3)	O1—Ru2—N5	83.9(4)
O1—Ru1—O5	83.7(3)	O2—Ru2—N7	92.2(4)
O1—Ru1—O6	103.5(3)	O2—Ru2—N5	93.7(4)
O3—Ru1—O5	173.4(4)	O6—Ru2—N7	86.5(4)
O3—Ru1—O6	82.8(3)	O6—Ru2—N5	170.5(4)
O1—Ru1—N1	168.6(4)	O4—Ru2—N7	92.2(4)
O1—Ru1—N3	85.4(4)	O4—Ru2—N5	89.8(4)
O5—Ru1—N1	91.3(4)	O1—Ru2—O4	83.3(4)
O5—Ru1—N3	91.4(4)	O1—Ru2—O6	104.7(3)
N1—Ru1—N3	84.5(4)	O1—Ru2—O2	92.8(3)
O6—Ru1—N1	87.0(4)	O2—Ru2—O6	82.0(3)
O6—Ru1—N3	170.5(4)	O2—Ru2—O4	174.5(3)
O5—Ru1—O6	92.8(3)	O4—Ru2—O6	95.1(3)
O3—Ru1—N1	93.3(4)	N5—Ru2—N7	85.2(4)
O3—Ru1—N3	93.7(3)	Ru2—O1—C1	122.3(8)
O1—Ru1—O3	92.5(3)	Ru2—O2—C2	119.6(8)
Ru1—O1—C1	120.8(7)	Ru2—O4—C10	120.9(7)
Ru1—O3—C2	117.9(7)	Ru2—O6—C18	129.7(7)
Ru1—O5—C10	120.8(9)	O6—C18—O7	120(1)
Ru1—O6—C18	121.0(8)	O7—C18—C19	128(1)
O2—C2—O3	127(1)	O6—C18—C19	112(1)
O3—C2—C3	116(1)		
O2—C2—C3	117(1)		
O4—C10—O5	125(1)		
O4—C10—C11	118(1)		
O5—C10—C11	117(1)		

Table 6. Selected Bond Distances (Å) and Angles (deg) for **2a**

Ru1—Ru1'	2.493(2)	Ru1'—O4	2.033(6)
Ru1—O1	2.049(5)	Ru1—N1	2.032(7)
Ru1—O2	2.068(5)	Ru1—N3	2.028(8)
Ru1—O4	2.006(5)	O4—C9	1.368(12)
O1—C1	1.275(10)	O5—C9	1.188(11)
C1—O2'	1.270(10)	C9—C10	1.473(14)
C1—C2	1.476(10)		
Ru1—O4—Ru1'	76.2(2)	Ru1'—O2'—C1	121.2(5)
O4—Ru1—N3	85.2(3)	Ru1'—O4—C9	122.0(5)
O2—Ru1—N3	92.3(2)	O1—C1—O2'	124.9(7)
O2—Ru1—O4	81.6(2)	O4—C9—O5	123.6(9)
O1—Ru1—N1	91.8(2)	O5—C9—C10	124(1)
N1—Ru1—N3	85.9(3)	Ru1—O1—C1	120.2(5)
O4—Ru1—N1	169.1(3)	O1—C1—C2	117.2(7)
O2—Ru1—N1	92.5(3)	O2'—C1—C2	117.8(7)
O1—Ru1—N3	93.0(3)	Ru1—O4—C9	122.0(5)
O1—Ru1—O4	94.9(2)	O4—C9—C10	111.9(9)
O1—Ru1—O2	173.4(2)		

like OR or OH groups enhance d–d overlaps, resulting in shorter M–M distances. In addition, the three-atom bridging ligands at the axial sites (L_a) of the core also promote greater overlap of the metal d orbitals in giving stronger metal–metal bonds. The dichloro-bridged complex $\text{Ru}_2\text{Cl}_6(\text{PBu}_3)_4$ belongs to the structural type I and displays⁵ a Ru–Ru separation which is much longer than that observed in $\text{Ru}_2\text{Cl}_6(\text{Me}_2\text{PCH}_2\text{PMe}_2)_2$ with a type II structure. $\text{Ru}_2\text{Cl}_6(\text{PBu}_3)_4$ is known⁵ to be paramagnetic while other d^5 – d^5 ESBO complexes are diamagnetic. Interest-

Table 7. ESBO d⁵-d⁵ Diruthenium Complexes

complex	Ru—Ru, Å	Ru—X—Ru, deg	ref
[Ru ₂ Cl ₆ (PBu ₃) ₄]	3.733(2)	98.75(9) (X = Cl)	5
[Ru ₂ Cl ₆ (Me ₂ PC ₂ H ₅ PM ₂) ₂]	2.933(1)	77.48(6) (X = Cl)	6
[Ru ₂ (NH ₂) ₂ (NH ₃) ₈]Cl ₄ ·4H ₂ O	2.625(1)	81.0(1) (X = N)	7
[Ru ₂ (C ₅ NH ₄ NH) ₆ (PM ₂ Ph) ₂]	2.573(2)	75.8(3) (X = N)	8
[Ru ₂ (p-C ₆ H ₄ CH ₃) ₂ (PhCONH) ₂ {(p-C ₆ H ₄ CH ₃) ₂ POC(Ph)N} ₂]	2.570(2)	77.3(3) (X = N)	9a
[Ru ₂ (Ph) ₂ {3,5-(OMe) ₂ C ₆ H ₃ CONH} ₂ {Ph ₂ POC(3,5-(OMe) ₂ C ₆ H ₃)N} ₂]	2.566(1)	78.4(2) (X = N)	9a
[Ru ₂ (Ph) ₂ (PhCONH) ₂ {Ph ₂ POC(Ph)N} ₂]	2.566(1)	78.4(2) (X = N)	9b
[Ru ₂ (OH) ₂ (CH ₃ CN) ₂ (η ⁵ -C ₅ H ₅)Co(P(O)(OCH ₃) ₂) ₂](CF ₃ SO ₃) ₂	2.622(1)	81.5(1) (X = O)	10
[Ru ₂ (OH) ₂ (HCOO)(η ⁵ -C ₅ H ₅)Co(P(O)(OCH ₃) ₂) ₂](CF ₃ SO ₃) ₂ ·2H ₂ O	2.548(1)	79.8(2) (X = O)	10
[Ru ₂ (OMe)(O ₂ CC ₆ H ₄ -p-OMe) ₃ (1-MeIm) ₄](PF ₆) ₂ ·1.5MeCN·0.5Et ₂ O	2.490(2)	75.9(3) (X = O)	this work
[Ru ₂ (O ₂ CC ₆ H ₄ -p-OMe) ₄ (1-MeIm) ₄](ClO ₄) ₂	2.493(2)	76.2(2) (X = O)	this work

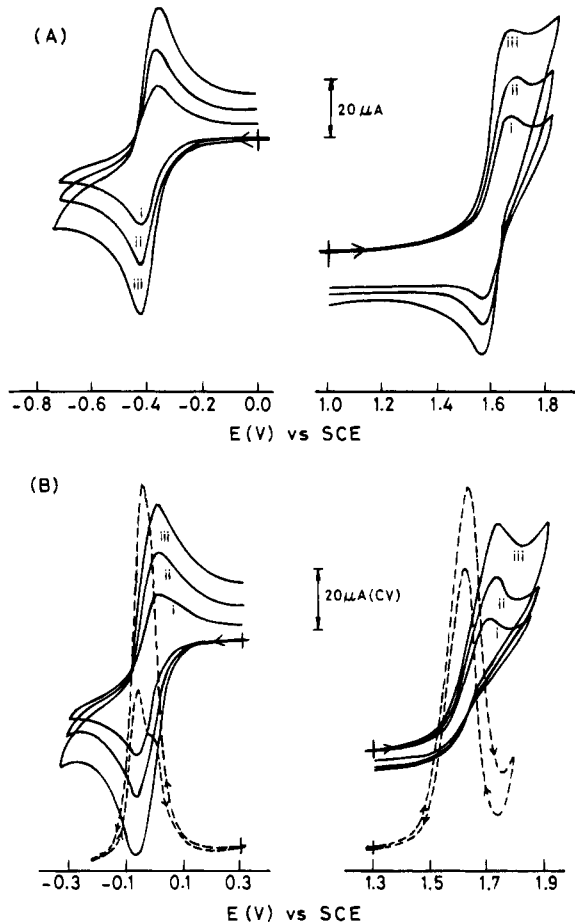


Figure 4. Cyclic voltammograms for the redox couples in (A) [Ru₂(OMe)(O₂CC₆H₄-p-Me)₃(1-MeIm)₄](ClO₄)₂ (**1b**) and (B) [Ru₂(O₂CC₆H₄-p-Me)₄(1-MeIm)₄]₂ (**2b**) in MeCN-0.1 M TBAP at scan rates (i) 20, (ii) 50, and (iii) 100 mV s⁻¹ along with the differential pulse voltammograms (---) for **2b** at 2 mV s⁻¹ (B).

ingly, the Ru—Ru distance in d⁵-d⁵ **1a'** and **2a** is comparable with the formal M—M double bond distances known¹ in dialkoxo-bridged d²-d² and d³-d³ systems.

Electrochemistry. The redox properties of complexes **1** and **2** have been studied by cyclic and differential pulse voltammetry in MeCN-0.1 M TBAP. The electrochemical data are given in Table 2. Complexes **1a** and **1b** undergo a reversible one-electron reduction near -0.4 V and a reversible one-electron oxidation at +1.6 V vs SCE (Figure 4). Cyclic voltammograms recorded for scan rates of 20–200 mV s⁻¹ show ΔE_p values of 60 mV for the reduction and 65 mV for the oxidation process with i_{pc} ≈ i_{pa}. The couples involved are given in eq 1. While the Ru^{III}, Ru^{III} → Ru^{III}, Ru^{IV} process leads to the formation of a mixed-valence species with a Ru—Ru bond order of 1.5, the addition of an electron to the σ* level gives a mixed-valence core having a Ru—Ru bond order of 0.5.

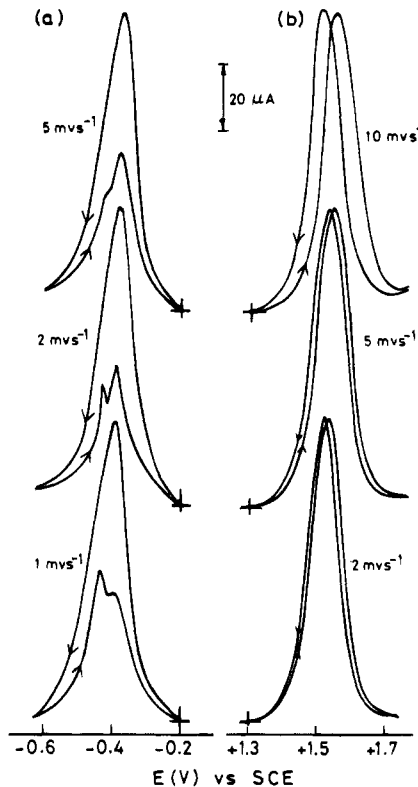
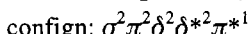
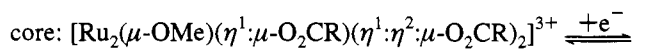
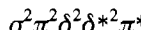
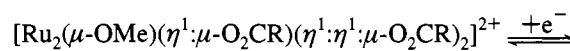


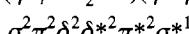
Figure 5. Differential pulse voltammograms at different scan rates for the redox couples in [Ru₂(OMe)(O₂CC₆H₄-p-OMe)₃(1-MeIm)₄](ClO₄)₂ (**1a**) in MeCN-0.1 M TBAP.



bond order: 1.5



1.0



0.5

The tetracarboxylate-bridged complexes **2a** and **2b** also undergo a reversible one-electron reduction process near -0.05 V and display a one-electron anodic cyclic voltammetric response near 1.7 V vs SCE with an unresolved cathodic counterpart (Figure 4). A cathodic peak with a diminished peak height is, however, observed in the differential pulse voltammogram of **2**. The couples involved in **2** are similar to those in **1** (eq 1). It is apparent from the electrochemical data that the HOMO and LUMO energy levels of the ESBO complexes are sensitive to the nature of the monoatomic bridges. A

substitution at the phenyl ring of the carboxylate ligand shows only the inductive effect of the substituent on the $E_{1/2}$ values. A large positive shift of $E_{1/2}$ is observed on changing the methoxy in **1** to the monoatomic carboxylate bridge in **2**. It implies that the σ^* level of **2** is more readily accessible for reduction than that of **1**. However, the π^* levels of **1** and **2** are essentially of similar energies. This indicates that the σ^* level is relatively more sensitive to the nature of L_b than the π^* level.

The study on the stability of the dimeric core is an interesting aspect of the chemistry of ESBO complexes. The cyclic voltammetric data on **1** and **2** show a HOMO–LUMO gap of ~2.0 V and the reversible nature of the electron-transfer processes involving π^* and σ^* orbitals. However, the differential pulse voltammograms for **1** at various scan rates show that the reduced species is less stable than the oxidized one (Figure 5). The ratio of backward- to forward-scan peak currents (I_{bs}/I_{fs}) for the reduction process decreases on reducing the scan rate, and the voltammogram for the reverse scan displays more than a single peak (Figure 5a). A 90 mV peak width at half height (δ) for the forward-scan voltammogram suggests the reversible nature of the electron transfer. Such an observation is indicative of the limited stability of the reduced species which becomes susceptible to chemical conversion (EC mechanism²²). This is possibly due to the addition of an electron to the σ^* level, which reduces the strength of the Ru–Ru σ

bond. The voltammograms for the oxidation process, however, show the I_{bs}/I_{fs} ratio of unity at all scan rates for **1** (Figure 5b).

Conclusions

Symmetrically and asymmetrically bridged ESBO diruthenium(III) complexes have been isolated from a novel core conversion reaction of $\text{Ru}_2\text{Cl}(\text{O}_2\text{CR})_4$. The ESBO core is found to be redox-active for oxidation and reduction over a wide range of potential. The addition of an electron to the σ^* level has been found to be easier than the removal of an electron from the π^* level of the complexes having a $\sigma^2\pi^2\delta^2\delta^{*2}\pi^{*2}$ electronic configuration. An increase in the metal–metal separation resulting from the addition of an electron to the σ^* level is found to be less favorable in the presence of a less bulky and more electron-donating monoatomic bridging ligand. The stability of the core and the reversibility of the electron-transfer process thus depend on both steric and electronic effects of the monoatomic bridging ligands in addition to the presence of three-atom bridging ligands.

Acknowledgment. We thank the Department of Science and Technology, Government of India, for financial support.

Supplementary Material Available: Tables listing additional crystallographic data, hydrogen atom coordinates, bond distances, bond angles, and anisotropic thermal parameters for $[\text{Ru}_2(\text{OMe})(\text{O}_2\text{CC}_6\text{H}_4-p\text{-OMe})_3(1\text{-MeIm})_4](\text{PF}_6)_2 \cdot 1.5\text{MeCN} \cdot 0.5\text{Et}_2\text{O}$ and $[\text{Ru}_2(\text{O}_2\text{CC}_6\text{H}_4-p\text{-OMe})_4(1\text{-MeIm})_4](\text{ClO}_4)_2$ (25 pages). Ordering information is given on any current masthead page.

(22) Nicholson, R. S.; Shain, I. *Anal. Chem.* **1964**, *36*, 706.